Bilateral Teleoperation for Linear Force Sensorless 3D Robots

Stefan Lichiardopol, Nathan van de Wouw, and Henk Nijmeijer

Dept. of Mechanical Engineering, Eindhoven University of Technology, PO Box 513, 5600 MB Eindhoven, The Netherlands
{s.lichiardopol,n.v.d.wouw,h.nijmeijer}@tue.nl

Abstract. It is well known that for bilateral teleoperation, force feedback information is needed. In this paper, we propose a control approach for bilateral teleoperation with uncertainties in the model of the slave robot and which does not use force sensors for haptic feedback. The controller design is based on a cyclic switching algorithm. In the first phase of the cyclic algorithm, we estimate the environmental force acting on the slave robot and in the second phase a tracking controller ensures that the position of the slave robot is tracking the position of the master robot. A stability analysis of the overall closed-loop system is presented and the approach is illustrated by means of an example.

Keywords: Bilateral teleoperation, Force sensor-less robotic setups, Haptic feedback.

1 Introduction

In this paper, we consider the problem of bilateral teleoperation in force-sensor-less robotic setups. It is well-known that haptic robotic devices and teleoperation systems exploit information regarding the external forces (see [1] and [2]), e.g. for haptic feedback. The slave robot interacts with the environment and its dynamics are dependent on external forces induced by this interaction. These forces can be contact forces (interaction forces between environmental objects and the robot) or exogenous forces induced by the environment.

In bilateral teleoperation, knowledge on the unknown environmental force applied on the slave robot is typically needed to achieve coordinated teleoperation. One option for obtaining such disturbance information is to equip the slave robot with force-sensors; for examples of such robotic devices, especially haptic devices, which use force sensors the reader is referred to [1], [3]. However, in many cases, the most important external forces for multi-link robots appear at the end-effector. Note that force sensing at the end effector of the robot is often not feasible since the external forces will typically interact with the load, which the slave robot is positioning, and not directly with the robot end-effector. Besides, in some cases, the position at which the external forces are applied is a priori unknown and may be on a robot link as opposed to on the end-effector. Moreover, the usage of force-sensors can be expensive and increase the production costs of the robot which can be undesirable especially in domestic applications.

J.A. Cetto et al. (Eds.): Informatics in Control, Automation and Robotics, LNEE 89, pp. 197–210.
springerlink.com

For these reasons, the usage of a disturbance estimation scheme for force-sensorless robots for the purpose of haptic feedback can be interesting. Disturbance observers (DOB) have been widely used in different motion control applications ([4], [5], [6]) for determining disturbance forces, such as friction forces. However, the performance enhancement of these DOB strategies may lead to smaller stability margins for the motion control ([7]); therefore, a robust design with respect to the environmental disturbances and model uncertainties is needed. Previous results on robustly stable DOB ([8], [9], [10], [11]) are based on linear robust control techniques. Some nonlinear DOB have been developed for the estimation of harmonic disturbance signals ([12], [13]).

Various strategies have also been considered for force-sensor-less control schemes estimating the external force. [14] proposes an adaptive disturbance observer scheme, and [15] and [16] propose an H^{∞} estimation algorithm. In [17], a control strategy called "force observer" is introduced. This design uses an observer-type algorithm for the estimation of the exogenous force. The drawback of this approach is that it assumes perfect knowledge of the model of the system.

In parallel with force estimation strategies, based on disturbance observers, another approach using sensor fusion has been developed to diminish the noise levels of the force sensors. In [18], force and acceleration sensors are used, while in [19], data from force sensors and position encoders are fused. Sensor fusion provides better qualitative results than obtained by employing more expensive force sensors.

Here, we present a control approach for bilateral teleoperation with an estimation strategy for external forces acting on the slave robot with a load with unknown mass. The difficulty in this solving this problem is that due to the uncertainties in the mass of the load it is possible for the previously referenced algorithms to estimate the exogenous force acting upon the slave robot. The method introduced in this chapter extends a result presented in [20], which considered the human-robotic co-manipulation problem. The proposed algorithm is robust for large uncertainties in the mass of the load.

The chapter is structured as follows. Section 2 presents the problem formulation and in Section 3 we describe the control strategy we propose. In Section 4, we apply the algorithm to a master-slave robotic setup. In the final section of the paper, the conclusions and some perspectives on future work are discussed.

2 Problem Statement

The problem that is tackled in this paper is that of bilateral teleoperation in force sensorless robotic setups. We assume that the slave robot is generally carrying a load (e.g. tool or product) and that the exogenous forces act on the slave or on the load. We consider the case in which no force sensor is present to measure the exogenous force directly. Moreover, we consider the realistic case in which the mass of the load is not known exactly which further challenges the estimation of the exogenous force. In order to solve this problem, we propose the design of a force estimator which is robust to the uncertainties in the mass of the load. In order to achieve teleoperation, the position of the slave robot must track the position of the master robot.

In Figure 1, the block diagram of the teleoperation setup is presented with the blocks $Master$ and $Slave$ representing the dynamics of the master and the slave robot, respectively, and the block C representing the control algorithm for bilateral teleoperation.

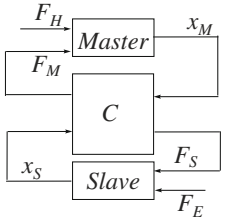

Fig. 1. Problem Setup.

The signals F_H and F_E represent the human and the environmental force, respectively; x_M and x_S are the positions of the master and the slave robots and F_M and F_S are the control signals for the master and slave robots, respectively. We adopt the assumption that the only measurements available are the position of the end-effectors and hence we aim to construct an output-feedback control strategy.

Consider the dynamics of the master and slaves robots dynamics:

$$\begin{cases} m_M \ddot{x}_M = F_H(t) + F_M(t) \\ m_S \ddot{x}_S = F_E(t) + F_S(t) \end{cases}, \tag{1}$$

where $x_M, x_S \in \mathbb{R}^3$ are the position of the master and the slave robots, respectively, $F_H, F_E \in \mathbb{R}^3$ are the human and the environmental force, respectively, m_M is the unknown inertia of the master robot (including some unknown inertia of the human hand) and m_S is the unknown inertia of the slave with the load (the masses are assumed to be bounded by $m_M, m_S \in [M_{min}, M_{max}]$).

The objective of this work is to design the controller C such that the following goals are met:

- the position of the slave robot is tracking the position of the master robot;
- an accurate estimate of the environmental force is transmitted to the master robot;
- the overall system is stable.

3 Control Design

Due to the uncertainties in the model of the slave robot we can not estimate the unknown environmental force and track the master robot position at the same time (the unknown inertia of the load and the fact that only position measurement data is available do not allow for simultaneous force estimation and position tracking). Therefore, we are proposing a switching controller based on a cyclic algorithm. During one cycle of duration T, we will have two phases as in Figure 2:

1. estimation of the environmental force;
2. position tracking.

During the first phase, which last for a period of T_0 ($T_0 < T$), the controller will behave as a force estimator. Here we are using the force observer introduced in [20] to estimate the external force which will be used for the purpose of haptic feedback

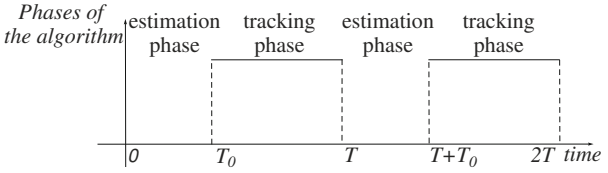

Fig. 2. Temporal division of the control strategy.

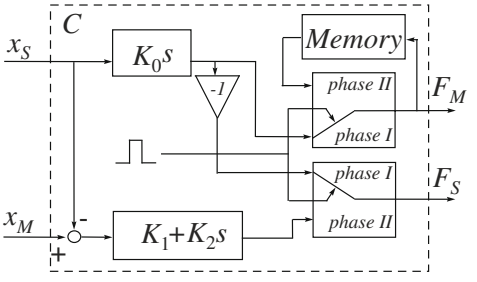

Fig. 3. Controller Design.

and during the second phase we are keeping the estimated force constant, $F_M(t) = \hat{F}_E(t) = K_0\dot{x}_S$ and $F_S(t) = -K_0\dot{x}_S$, for $kT \leq t < kT + T_0$, $k \in \mathbb{N}$, where parameter K_0 is a scalar parameter in the force estimation algorithm and is chosen such that the settling time of the estimation of the force is smaller than T_0. In the second phase, we are using a PD controller for the slave robot to track the position of the master robot, $F_M(t) = \hat{F}_E(kT + T_0)$ and $F_S(t) = K_1(x_M - x_S) + K_2(\dot{x}_M - \dot{x}_S)$, for $kT + T_0 \leq t < (k+1)T$, $k \in \mathbb{N}$, where scalars K_1 and K_2 represent parameters of the PD controller that ensures the tracking of the master robot position by the slave robot (these parameters are chosen such that the polynomial $m_S s^2 + K_2 s + K_1$ is Hurwitz $\forall m_S \in [M_{min}, M_{max}]$) and $\hat{F}_E(KT+T_0)$ is the estimation of the environmental force at the end of the first phase. In Figure 3, we present the block diagram representation of the controller where the controller blocks are represented by their transfer functions in the Laplace domain ($s \in \mathbb{C}$) and the block called $Memory$ saves the last estimate of the environmental force at the end of the first phase and provides the same constant output during the entire second phase.This means that (estimation phase) and (tracking phase). The switches in Figure 3 are set on positions corresponding to the first phase of the algorithm.

In the following section, we study the stability for the closed-loop system (including force estimation error dynamics and tracking error dynamics).

3.1 Description of Model Dynamics

For the purpose of stability analysis, we first formulate the model of the error dynamics. In order to obtain the error dynamics, the dynamics of the master and slaves robots are needed in both phases. During the first phase ($kT \leq t < kT + T_0$, $k \in \mathbb{N}$), the model dynamics are:

$$\begin{cases} m_M \ddot{x}_M = F_H(t) + K_0 \dot{x}_S \\ m_S \ddot{x}_S = F_E(t) - K_0 \dot{x}_S \end{cases}. \tag{2}$$

In the second phase of the algorithm ($kT + T_0 \leq t < (k+1)T$, $k \in \mathbb{N}$), the system behavior is described by:

$$\begin{cases} m_M \ddot{x}_M = F_H(t) + \hat{F}_E(kT + T_0) \\ m_S \ddot{x}_S = F_E(t) + K_1(x_M - x_S) + K_2(\dot{x}_M - \dot{x}_S) \end{cases}. \tag{3}$$

In the sequel, we assume that the exogenous forces acting on the system (human force $F_H(t)$ and environmental force $F_E(t)$) and their derivatives are bounded.

Given the fact that the same world frame is considered for both master and slave robots, the 3D system described by relations (2) and (3) can be seen as a set of three decoupled 1-DOF systems along each space dimension. Since the behavior for the three 1-dof system is similar, for simplicity, we are going to consider in the sequel only 1-DOF system, knowing that the extension for 3D systems is trivial.

3.2 Stability Analysis

Let us define the vector of tracking error coordinates $\epsilon = [e_x, \dot{e}_x]^T = [x_M(t) - x_S(t), \dot{x}_M(t) - \dot{x}_S(t)]^T$, which contains both the position and the velocity tracking errors, and the force estimation error $e_F = \hat{F}_E - F_E$. Then the force estimation error dynamics are described by:

$$\dot{e}_F = -\frac{K_0}{m_S} e_F - \dot{F}_E, \tag{4}$$

during the first step of the algorithm ($kT \leq t < kT + T_0$, $k \in \mathbb{N}$) and

$$\dot{e}_F = -\dot{F}_E, \tag{5}$$

during the second phase ($kT + T_0 \leq t < (k+1)T$, $k \in \mathbb{N}$).

The tracking error dynamics is represented by:

$$\dot{\epsilon} = \begin{pmatrix} 0 & 1 \\ 0 & 0 \end{pmatrix} \epsilon + \begin{pmatrix} 0 & 0 \\ \frac{1}{m_M} & \frac{1}{m_M} \end{pmatrix} \begin{pmatrix} F_H \\ F_E \end{pmatrix} + \begin{pmatrix} 0 \\ \frac{1}{m_M} + \frac{1}{m_S} \end{pmatrix} e_F, \tag{6}$$

for $t \in [kT, kT + T_0)$, with $k \in \mathbb{N}$ and

$$\dot{\epsilon} = \begin{pmatrix} 0 & 1 \\ -\frac{K_1}{m_S} & -\frac{K_2}{m_S} \end{pmatrix} \epsilon + \begin{pmatrix} 0 & 0 \\ \frac{1}{m_M} & \frac{1}{m_M} - \frac{1}{m_S} \end{pmatrix} \begin{pmatrix} F_H \\ F_E \end{pmatrix} + \begin{pmatrix} 0 \\ \frac{1}{m_M} \end{pmatrix} e_F, \tag{7}$$

for $t \in [kT + T_0, (k+1)T)$, with $k \in \mathbb{N}$.

The goal of this section is to prove that the composed estimation and tracking error dynamics (4)-(7) are input-to-state stable with respect to the inputs F_H, F_E and $\dot{F}_E$. For this we are going to use a result introduced in [21] that states that the series connection of two input-to-state stable systems is also an input-to-state stable system. In the sequel, this proof will be split into two parts:

- first, we prove that the force error dynamics (4), (5) are input-to-state stable with respect to the input $\dot{F}_E$;
- secondly, we prove that the tracking error dynamics (6), (7) are input-to-state stable with respect to the inputs F_H, F_E and e_F.

Input-to-State Stability of the Force Estimation Error Dynamics. The stability analysis of the force estimation error dynamics is done by studying an exact discretisation of the system (4), (5) at the sampling instances kT. Let us now construct such a discrete-time model.

The solution of system (4) at time $t = kT + T_0$, with $k \in \mathbb{N}$, is:

$$e_F(kT + T_0) = e^{-\frac{K_0}{m_S}T_0} e_F(kT) + + \int_0^{T_0} e^{-\frac{K_0}{m_S}(T_0-\tau)} \dot{F}_E(kT + \tau)d\tau. \tag{8}$$

The solution of system (5) at time $t = (k + 1)T$, with $k \in \mathbb{N}$, is:

$$e_F((k + 1)T) = e_F(kT + T_0) - \int_0^{T-T_0} \dot{F}_E(kT + T_0 + \tau)d\tau. \tag{9}$$

Define the sampled force estimation error by $e_k := e_F(kT)$, with $k \in \mathbb{N}$. Combining relations (8) and (9), one can obtain the discrete-time force estimation error dynamics:

$$e_{k+1} = e^{-\frac{K_0}{m_S}T_0} e_k + w_k, \tag{10}$$

with $w_k = \int_0^{T_0} e^{-\frac{K_0}{m_S}(T_0-\tau)} \dot{F}_E(kT+\tau)d\tau - \int_0^{T-T_0} \dot{F}_E(kT+T_0+\tau)d\tau$. The system (10) is input-to-state stable with respect to the input w_k because $\left|e^{-\frac{K_0}{m_S}T_0}\right| < 1$, since the parameters K_0, T_0 and the inertia m_S are positive. Note that w_k is bounded for any bounded $\dot{F}_E(t)$ and bounded T_0.

Now we exploit a result in [22] that says that if the discrete-time dynamics is ISS and the intersample behavior is uniformly globally bounded over T, then the corresponding continuous-time dynamics is ISS. The fact that the intersample behavior is uniformly globally bounded over T directly follows from (4), (5) with $\dot{F}_E$ bounded, since

$$e(t) = \begin{cases} e^{-\frac{K_0}{m_S}(t-kT)} e_F(kT) + \int_{kT}^{t} e^{-\frac{K_0}{m_S}(t-\tau)} \dot{F}_E(\tau)d\tau\,, & kT \le t < kT + T_0 \\ e_F(kT + T_0) - \int_{kT+T_0}^{t} \dot{F}_E(\tau)d\tau\,, & kT + T_0 \le t < (k + 1)T \end{cases}. \tag{11}$$

Input-to-State Stability of the Tracking Error Dynamics. Similarly to the study of the force estimation error dynamics, we evaluate the input-to-state stability property of the tracking error dynamics with respect to the inputs F_H, F_E and e_F.

The solution of system (6) at time $t = kT + T_0$, with $k \in \mathbb{N}$, is:

$$\begin{aligned} \epsilon(kT + T_0) = e^{A_1 T_0}\epsilon(kT) + \int_0^{T_0} e^{A_1(T_0-\tau)} B_{11} u(kT + \tau)d\tau \\ + \int_0^{T_0} e^{A_1(T_0-\tau)} B_{12} e_F(kT + \tau)d\tau, \end{aligned} \tag{12}$$

where $A_1 = \begin{pmatrix} 0 & 1 \\ 0 & 0 \end{pmatrix}$, $B_{11} = \begin{pmatrix} 0 & 0 \\ \frac{1}{m_M} & \frac{1}{m_M} \end{pmatrix}$, $B_{12} = \begin{pmatrix} 0 \\ \frac{1}{m_M} + \frac{1}{m_S} \end{pmatrix}$ and $u(t) = \begin{pmatrix} F_H(t) \\ F_E(t) \end{pmatrix}$.

The solution of system (7) at time $t = (k + 1)T$, with $k \in \mathbb{N}$, is:

$$\begin{aligned} \epsilon((k + 1)T) = e^{A_2(T-T_0)}\epsilon(kT + T_0) + \int_0^{T-T_0} e^{A_2(T-T_0-\tau)} B_{21} u(kT + T_0 + \tau)d\tau \\ + \int_0^{T-T_0} e^{A_2(T-T_0-\tau)} B_{22} e_F(kT + T_0 + \tau)d\tau, \end{aligned} \tag{13}$$

where $A_2 = \begin{pmatrix} 0 & 1 \\ -\frac{K_1}{m_S} & -\frac{K_2}{m_S} \end{pmatrix}$, $B_{21} = \begin{pmatrix} 0 & 0 \\ \frac{1}{m_M} & \frac{1}{m_M} - \frac{1}{m_S} \end{pmatrix}$ and $B_{22} = \begin{pmatrix} 0 \\ \frac{1}{m_M} \end{pmatrix}$.
Let us define

$$\omega_k := e^{A_2(T-T_0)}(\int_0^{T_0} e^{A_1(T_0-\tau)}B_{11}u(kT+\tau)d\tau + \int_0^{T_0} e^{A_1(T_0-\tau)}B_{12}e_F(kT+\tau)d\tau) + \int_0^{T-T_0} e^{A_2(T-T_0-\tau)}B_{21}u(kT+T_0+\tau)d\tau + \int_0^{T-T_0} e^{A_2(T-T_0-\tau)}B_{22}e_F(kT+T_0+\tau)d\tau \tag{14}$$

and $\epsilon_k := \epsilon(kT)$, with $k \in \mathbb{N}$. Combining relations (12) and (13), we obtain the following discrete-time error dynamics:

$$\epsilon_{k+1} := e^{A_2(T-T_0)}e^{A_1T_0}\epsilon_k + \omega_k, \tag{15}$$

where ω_k is bounded for all k, since T, T_0 are bounded, F_E, F_H are bounded by assumption and e_F is bounded due to the fact that the force estimation error dynamics is ISS with respect to $\dot{F}_E$.

Next, we study the input-to-state stability property of the system (15) with respect to the input ω_k. But before we carry out this step, we need to evaluate the matrix $Q = e^{A_2(T-T_0)}e^{A_1T_0}$. Namely, input-to-state stability of (15) implies, firstly, the global uniform asymptotic stability of $\epsilon = 0$ when the input ω_k is zero and the boundness of the error ϵ for bounded inputs ω_k.

For the evaluation of the matrix Q, two exponential matrices must be determined; as the matrix A_1T_0 depends only on known parameters, we can easily determine its exponential:

$$E_1 := e^{A_1T_0} = \begin{pmatrix} 1 & T_0 \\ 0 & 1 \end{pmatrix}. \tag{16}$$

In order to compute the exponential of matrix $P = A_2(T-T_0)$, we are using a procedure similar to the one introduced in [23], which employs the Cayley-Hamilton theorem, which says that if $p(\lambda) = \det(\lambda I_n - A)$, with I_n the $n \times n$ identity matrix, is the characteristic polynomial of a matrix $A \in \mathbb{R}^{n\times n}$ then $p(A) = 0$. This means that given the matrix P, for any $i \geq 2$, there exists a set of coefficients $a_i, b_i \in \mathbb{R}$ such that the i^{th} power of P can be expressed in terms of its first two powers:

$$P^i = a_iI_n + b_iP. \tag{17}$$

Let us now exploit (17) to determine the exponential of the matrix P:

$$e^P = \sum_{i=0}^{\infty} \frac{P^i}{i!} = \sum_{i=0}^{\infty} \frac{1}{i!}(a_iI_2 + b_iP), \tag{18}$$

or

$$e^P = \left(\sum_{i=0}^{\infty} \frac{a_i}{i!}\right) I_2 + \left(\sum_{i=0}^{\infty} \frac{b_i}{i!}\right) P. \tag{19}$$

Using the expression of A_2, we can decompose P as follows: $P = U + \frac{1}{m_S}L$, where

$$U = \begin{pmatrix} 0 & T-T_0 \\ 0 & 0 \end{pmatrix} \tag{20}$$

and

$$L = \begin{pmatrix} 0 & 0 \\ -K_1(T-T_0) & -K_2(T-T_0) \end{pmatrix}. \tag{21}$$

Consequently, the expression for the exponential matrix becomes:

$$e^P = \left(\sum_{i=0}^{\infty} \frac{a_i}{i!}\right) I_2 + \left(\sum_{i=0}^{\infty} \frac{b_i}{i!}\right) U + \frac{1}{m_S}\left(\sum_{i=0}^{\infty} \frac{b_i}{i!}\right) L. \tag{22}$$

Let us now define the following scalars:

$$\underline{\alpha} = \min_{m_S \in [M_{min}, M_{max}]} \left(\sum_{i=0}^{\infty} \frac{a_i}{i!}\right), \tag{23}$$

$$\overline{\alpha} = \max_{m_S \in [M_{min}, M_{max}]} \left(\sum_{i=0}^{\infty} \frac{a_i}{i!}\right), \tag{24}$$

$$\underline{\beta} = \min_{m_S \in [M_{min}, M_{max}]} \left(\sum_{i=0}^{\infty} \frac{b_i}{i!}\right), \tag{25}$$

and

$$\overline{\beta} = \max_{m \in [M_{min}, M_{max}]} \left(\sum_{i=0}^{\infty} \frac{b_i}{i!}\right). \tag{26}$$

Given the fact that $m_S \in [M_{min}, M_{max}]$, we can define the scalars $\underline{\gamma} = \frac{1}{M_{max}}$ and $\overline{\gamma} = \frac{1}{M_{min}}$.

Then there always exist $\zeta_1, \zeta_2, \zeta_3 \in [0, 1]$ such that:

$$\left(\sum_{i=0}^{\infty} \frac{a_i}{i!}\right) = \zeta_1 \underline{\alpha} + (1 - \zeta_1)\overline{\alpha}, \tag{27}$$

$$\left(\sum_{i=0}^{\infty} \frac{b_i}{i!}\right) = \zeta_2 \underline{\beta} + (1 - \zeta_2)\overline{\beta} \tag{28}$$

and

$$\frac{1}{m_S} = \zeta_3 \underline{\gamma} + (1 - \zeta_3)\overline{\gamma}. \tag{29}$$

Introducing relations (27), (28) and (29) into expression (22) leads to:

$$\begin{aligned} e^P = &\left(\zeta_1 \underline{\alpha} + (1 - \zeta_1)\overline{\alpha}\right) I_2 + \left(\zeta_2 \underline{\beta} + (1 - \zeta_2)\overline{\beta}\right) U \\ &+ \left(\zeta_3 \underline{\gamma} + (1 - \zeta_3)\overline{\gamma}\right)\left(\zeta_2 \underline{\beta} + (1 - \zeta_2)\overline{\beta}\right) L, \end{aligned} \tag{30}$$

for some $\zeta_1, \zeta_2, \zeta_3 \in [0, 1]$.

Let us define the matrices $\Gamma_1 = 3\underline{\alpha}E_1$, $\Gamma_2 = 3\overline{\alpha}E_1$, $\Gamma_3 = 3\underline{\beta}UE_1$, $\Gamma_4 = 3\overline{\beta}UE_1$, $\Gamma_5 = 3\underline{\beta}\underline{\gamma}LE_1$, $\Gamma_6 = 3\underline{\beta}\overline{\gamma}LE_1$, $\Gamma_7 = 3\overline{\beta}\underline{\gamma}LE_1$ and $\Gamma_8 = 3\overline{\beta}\overline{\gamma}LE_1$, and the scalars $\varrho_1 = \frac{\zeta_1}{3}$, $\varrho_2 = \frac{1-\zeta_1}{3}$, $\varrho_3 = \frac{\zeta_2}{3}$, $\varrho_4 = \frac{1-\zeta_2}{3}$, $\varrho_5 = \frac{\zeta_2\zeta_3}{3}$, $\varrho_6 = \frac{\zeta_2(1-\zeta_3)}{3}$, $\varrho_7 = \frac{(1-\zeta_2)\zeta_3}{3}$, $\varrho_8 = \frac{(1-\zeta_2)(1-\zeta_3)}{3}$. This means that the expression of matrix Q is equivalent to:

$$Q = \sum_{i=1}^{8} \varrho_i \Gamma_i, \tag{31}$$

with $\sum_{i=1}^{8} \varrho_i = 1$.

Thus we have now found the generators for a convex (polytopic) matrix set that overapproximates the matrix set Q, with the uncertain parameter $m_S \in [M_{min}, M_{max}]$. Notice that $\sum_{i=0}^{\infty} \frac{a_i}{i!}$ and $\sum_{i=0}^{\infty} \frac{b_i}{i!}$ are infinite sums and will in practice be approximated by finite sums of length N. Next, we provide an explicit upper bound on the 2-norm of the approximation error induced by such truncation.

Theorem 1. *Consider an integer $N \in \mathbb{N}$ and a real positive scalar ϑ such that*

- $\mu = \sqrt{\frac{\lambda_{max}}{\vartheta}} < 1$, *where*

$$\lambda_{max} = \max_{m_S \in [M_{min}, M_{max}]} \left\{ eig(P^T P) \right\}, \tag{32}$$

- $\forall i \geq N$, $\sqrt{\vartheta^i} < i!$.

Then:

$$\left\| \sum_{i=N}^{\infty} \frac{P^i}{i!} \right\|_2 \leq \frac{\mu^N}{1-\mu}. \tag{33}$$

Proof.

$$\left\| \sum_{i=N}^{\infty} \frac{P^i}{i!} \right\|_2 \leq \sum_{i=N}^{\infty} \left\| \frac{P^i}{i!} \right\|_2 \leq \sum_{i=N}^{\infty} \frac{\|P^i\|_2}{i!} \leq \sum_{i=N}^{\infty} \frac{\sqrt{(\lambda_{max})^i}}{i!}, \tag{34}$$

where the inequality $\|A^i\|_2^2 \leq \|A\|_2^2 \times \ldots \times \|A\|_2^2 = \max(eig((A^T A))^i$ has been used. Using the property that $\forall a \in \mathbb{R}^+$, $\exists N \in \mathbb{N}$ such that $\forall i \geq N$, $\sqrt{a^i} < i!$, inequality (34) becomes:

$$\left\| \sum_{i=N}^{\infty} \frac{P^i}{i!} \right\|_2 \leq \sum_{i=N}^{\infty} \frac{\sqrt{(\lambda_{max})^i}}{i!} \leq \sum_{i=N}^{\infty} \mu^i. \tag{35}$$

Let us now employ the known result of convergence of geometric series which states that $\forall a \in [0, 1)$, $\lim_{n\to\infty} \sum_{i=0}^{n} a^i = \lim_{n\to\infty} \frac{1-a^{n+1}}{1-a} = \frac{1}{1-a}$.

$$\left\| \sum_{i=N}^{\infty} \frac{P^i}{i!} \right\|_2 \leq \frac{\mu^N}{1-\mu}. \tag{36}$$

□

Using Theorem 1, we can choose N such that the approximation error is small (even as low as the machine accuracy).

In the next theorem, we provide LMI-based stability conditions for the discrete-time tracking error dynamics (15) to be ISS with respect to the input ω_k.

Theorem 2. *Consider the discrete-time system (15). If there exists a matrix $\Omega = \Omega^T > 0$ and scalar $\varsigma \in (0, 1)$, such that the following linear matrix inequalities are satisfied:*

$$\Gamma_i{}^T \Omega \Gamma_i - \Omega \leq -\varsigma \Omega, i \in \{1, \ldots, 8\}, \tag{37}$$

where Γ_i are defined above, then the system (15) is ISS with respect to the input ω_k.

Proof: Using the Schur complement, relations (37) can be written as:

$$\begin{pmatrix} -\Omega & {\Gamma_i}^T\Omega \\ \Omega\Gamma_i & -\Omega \end{pmatrix} \leq -\varsigma\Omega, i \in \{1,\ldots,8\}. \tag{38}$$

Multiplying every inequality (38) with ϱ_i and summing them up, we obtain:

$$\begin{pmatrix} -\Omega\sum_{i=1}^{8}\varrho_i & \sum_{i=1}^{8}\varrho_i{\Gamma_i}^T\Omega \\ \Omega\sum_{i=1}^{8}\varrho_i\Gamma_i & -\Omega\sum_{i=1}^{8}\varrho_i \end{pmatrix} \leq -\varsigma\Omega\sum_{i=1}^{8}\varrho_i, \tag{39}$$

which according to equation (31) is:

$$\begin{pmatrix} -\Omega & Q^T\Omega \\ \Omega Q & -\Omega \end{pmatrix} \leq -\varsigma\Omega, \tag{40}$$

or

$$Q^T\Omega Q - \Omega \leq -\varsigma\Omega. \tag{41}$$

Let the candidate ISS-Lyapunov function be $V_k = (\epsilon_k)^T\Omega\epsilon_k$. We compute $\triangle V_k = V_{k+1} - V_k$:

$$\triangle V_k = (\epsilon_k)^T Q^T\Omega Q\epsilon_k - (\epsilon_k)^T\Omega\epsilon_k + 2(\epsilon_k)^T Q^T\Omega\omega_k + (\omega_k)^T\Omega\omega_k, \tag{42}$$

which according to (41) gives:

$$\triangle V_k \leq -\varsigma(\epsilon_k)^T\Omega\epsilon_k + 2(\epsilon_k)^T Q^T\Omega\omega_k + (\omega_k)^T\Omega\omega_k \tag{43}$$

After some straightforward computations, we can show that:

$$\|\epsilon\|_2 \geq \frac{2}{\varsigma}\sqrt{\frac{\lambda_{max}}{\lambda_{min}}}\sup_{k\in\mathbb{N}}(\omega_k) \Rightarrow \triangle V \leq -\frac{\varsigma}{2}\|\epsilon\|_2^2, \tag{44}$$

where λ_{max} and λ_{min} are the largest and the smallest eigenvalues of matrix Ω, respectively.

(44) implies that system (15) is input-to-state stable with respect to the input ω_k; see [24] for sufficient conditions for the ISS of discrete-time systems.

Remark 1. *For the sake of simplicity, Theorem 2 is based on a common quadratic ISS Lyapunov function $V = \epsilon^T\Omega\epsilon$. Alternatively, a parameter-dependent Lyapunov function approach could straight-forwardly be exploited to formulate less conservative stability conditions.*

The LMIs (37) are defined for the non-truncated Γ_i, but in practice we evaluate the vertex matrices using a truncation after N iterations as provided by Theorem 1. The errors can be ensured to be as low as the machine accuracy by choosing N large enough, just as the errors obtained from the numerical solver of the LMIs.

The last part of the study of the ISS property of the tracking error dynamics is to analyze the intersample behavior. Using Theorem 2, we can prove that the error dynamics are ISS on the sampling instances $t = kT$, with $k \in \mathbb{N}$. Given the choice of the parameters K_1 and K_2 such that the system (7) is Hurwitz for all $m_S \in [M_{min}, M_{max}]$, we

can conclude that during the second phase ($t \in [kT + T_0, (k+1)T)$) the evolution of the tracking error is bounded. In order to prove the stability of the overall continuous-time system, we need to show that the position error dynamics are also bounded for $t \in (kT, kT + T_0)$.

The solution of system (6), for $t \in (kT, kT + T_0)$, is given by:

$$\begin{aligned}\epsilon(kT+t) = \begin{pmatrix} 1 & t \\ 0 & 1 \end{pmatrix} \epsilon(kT) + \int_0^t \begin{pmatrix} 1 & t-\tau \\ 0 & 1 \end{pmatrix} B_{11} u(kT+\tau) d\tau \\ + \int_0^t \begin{pmatrix} 1 & t-\tau \\ 0 & 1 \end{pmatrix} B_{12} e_F(kT+\tau) d\tau,\end{aligned} \tag{45}$$

with $t \in [0, T_0]$. As the human force and the environmental force are bounded, we can define $F = \max_{t \in (kT, kT+T_0)} (|F_H(t)| + |F_E(t)|)$. In the previous section, we have proven that the force estimation error dynamics are ISS and consequently $e_F(t)$ is bounded; therefore, there exists $E_F = \max_{t \in (kT, kT+T_0)} (|e_F(t)|)$, with E_F bounded. Considering the three terms in the right-hand side of (45), we can conclude that the first one is bounded due to the boundness of the discrete-time error dynamics and the fact that $t \in [0, T_0]$, the second term satisfies:

$$\left| \int_0^t \begin{pmatrix} 1 & t-\tau \\ 0 & 1 \end{pmatrix} B_{11} u(kT+\tau) d\tau \right| \leq \left| \frac{F}{m_M} \begin{pmatrix} \frac{T_0^2}{2} \\ T_0 \end{pmatrix} \right|, \tag{46}$$

and the third term satisfies:

$$\left| \int_0^t \begin{pmatrix} 1 & t-\tau \\ 0 & 1 \end{pmatrix} B_{12} e_F(kT+\tau) d\tau \right| \leq \left| \left(\frac{1}{m_M} + \frac{1}{m_S} \right) E_F \begin{pmatrix} \frac{T_0^2}{2} \\ T_0 \end{pmatrix} \right|. \tag{47}$$

Therefore, we can conclude that the inter-sample evolution of tracking error is also bounded for $t \in (kT, kT + T_0)$. Once more, we can employ the result from [22] to prove that the continuous-time tracking error dynamics (6), (7) is ISS with respect to the inputs F_H, F_E and e_F because the discrete-time tracking error dynamics is ISS and the intersample behavior is uniformly globally bounded over T.

Since the force estimation error dynamics (4), (5) is ISS with respect to the input $\dot{F}_E$ and the tracking error dynamics (6), (7) is ISS with respect to the inputs F_H, F_E and e_F, we use the result introduced by [21] concerning the series connection of ISS systems to conclude that the closed-loop system (4)-(7), see also Figure 1 with the controller C with the block diagram representation from Figure 3, is ISS with respect to the inputs F_H, F_E and $\dot{F}_E$.

Remark 2. *By studying the ISS property of the estimation and tracking error dynamics, one can observe that the steady-state force estimation and tracking errors can be influenced by tuning the parameters T, T_0, K_0, K_1 and K_2. The algorithm provides a deeper insight into these relations. If we consider the converging manifold that bounds the error signal we can determine these parameters in accordance with the desired convergence rate.*

Remark 3. *In case the environmental force F_E is constant, i.e. $\dot{F}_E = 0$, the force estimation dynamics are globally exponentially stable and the tracking error dynamics is ISS with respect to the inputs F_H and F_E. This means that "perfect" haptic feedback is provided and that bounded tracking errors remain; therefore the closed loop system is stable.*

Remark 4. *The exact "tracking" regulation of the slave robot with respect to what the human has in mind is up to the human (since the human is in charge of the ultimate positioning).*

4 An Illustrative Example

In this section, we will apply the control design proposed in the previous section to a master-slave teleoperation setup consisting of two 1-DOF robots. The inertia of the robots is considered to be in the range $m_M, m_S \in [0.1, 10]kg$.

The "human" controller has been emulated by a linear transfer function:

$$H(s) = \frac{K_d(T_d s + 1)}{T_{PL} s + 1} = \frac{500(1+s)}{0.1s + 1}, \tag{48}$$

with saturation at $\pm 100N$. Here we use real human parameters, since the human movement is lower than $6Hz$. Moreover, to comply with the human sensing range, which is between $0Hz$ and $40 - 400Hz$ depending on the amplitude of the input signal, we have chosen the parameters of the cycle period of the controller $T = 0.01s$ and the duration of the first stage $T_0 = T/2 = 0.005s$. The force estimator acting in the first phase of the algorithm is defined by parameter $K_0 = 10^5$. The tracking PD controller which is active during the second phase has the parameters $K_1 = 200$ and $K_2 = 1$.

In Figure 4, we present the results of the simulation of the master-slave position tracking when the "human" is performing a movement from $0m$ to $0.25m$ on the master robot (i.e. the "human" force F_H is computed such that this motion is achieved) and a sinusoidal external force $F_E(t) = 0.5sin(2\pi t)$ is disturbing the slave robot. The dotted line is the position of the master and the solid line is the position of the slave.

One can observe that because no disturbance rejection controller is implemented, the external force is preventing the position signal to settle exactly at $0.25m$. In Figure 5, a zoomed in version of the Figure 4 that emphasizes this aspect is presented.

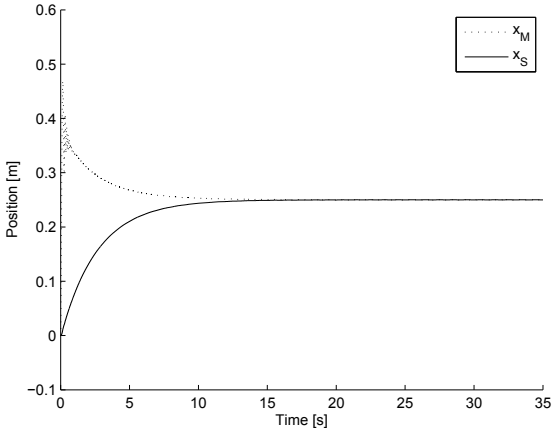

Fig. 4. Position tracking.

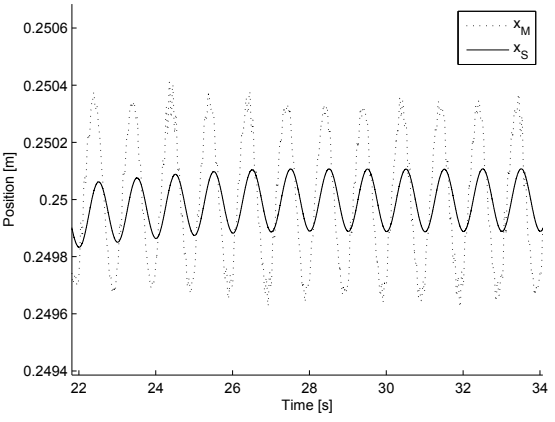

Fig. 5. Position tracking (zoomed version of Figure 4).

5 Conclusions and Perspectives

In this paper, we have introduced a new control algorithm for bilateral teleoperation of 3D robots in force-sensorless setups using a switching strategy between a force estimating controller and a tracking controller. This switching algorithm guarantees both the estimation of the environmental force acting upon the slave robot (to be used in haptic feedback) in the absence of force sensors and the convergence of the tracking errors in the case of external perturbations acting on the slave robot. We note that the ultimate position setting is the responsibility of the human, as he is in charge of the position of the master robot. Finally, we remark that the proposed algorithm is robust for an unknown inertia of the load to be carried by the slave robot and an unknown inertia of the human hand on the master side.

Future perspectives of this work will mainly focus on an extension to multi-degree-of-freedom robots with nonlinear dynamics. The reader should note that the extension of this result for robots with nonlinear dynamics using a pseudo-linearizing controller as in [20] is not straight forward, due to the variable change which depends on the velocities and accelerations.

References

1. Lawrence, D.: Stability and transparency in bilateral teleoperation. IEEE Transactions on Robotics and Automation 9, 624–637 (1993)
2. Hokayem, P.F., Spong, M.W.: Bilateral teleoperation: A historical survey. Automatica 42, 2035–2057 (2006)
3. Yokokohji, Y., Yoshikawa, T.: Bilateral control of master-slave manipulators for ideal kinematics coupling formulation and experiment. IEEE Transactions on Robotics and Automation 10, 605–620 (1994)
4. White, M.T., Tomizuka, M., Smith, C.: Improved track following in magnetic disk drives using a disturbance observer. IEEE Transactions on Mechatronics 5, 3–11 (1998)

5. Fujiyama, K., Katayama, R., Hamaguchi, T., Kawakami, K.: Digital controller design for recordable optical disk player using disturbance observer. In: Proceedings of the International Workshop on Advanced Motion Control, pp. 141–146 (2000)
6. Iwasaki, M., Shibata, T., Matsui, N.: Disturbance-observer-based nonlinear friction compensation in table drive system. IEEE Transactions on Mechatronics 4, 3–8 (1999)
7. Komada, S., Machii, N., Hori, T.: Control of redundant manipulators considering order of disturbance observer. IEEE Transactions on Industrial Electronics 47, 413–420 (2000)
8. Kempf, C.J., Kobayashi, S.: Disturbance observer and feedforward design for high-speed direct-drive position table. IEEE Transactions on Control System Technology 7, 513–526 (1999)
9. Eom, K.S., Suh, I.H., Chung, W.K.: Disturbance observer based path tracking of robot manipulator considering torque saturation. Mechatronics 11, 325–343 (2000)
10. Güvenc, B.A., Güvenc, L.: Robustness of disturbance observers in the presence of structured real parametric uncertainty. In: Proceedings of the American Control Conference, pp. 4222–4227 (2001)
11. Ryoo, J.R., Doh, T.Y., Chung, M.J.: Robust disturbance observer for the track-following control system of an optical disk drive. Control Engineering Practice 12, 577–585 (2004)
12. Chen, X., Komada, S., Fukuda, T.: Design of a nonlinear disturbance observer. IEEE Transactions on Industrial Electronics 47, 429–436 (2000)
13. Liu, C.S., Peng, H.: Disturbance observer based tracking control. Journal of Dynamic Systems, Measurement and Control 122, 332–335 (2000)
14. Eom, K.S., Suh, I.H., Chung, W.K., Oh, S.R.: Disturbance observer based force control of robot manipulator without force sensor. In: Proceedings of IEEE International Conference on Robotics and Automation, pp. 3012–3017 (1998)
15. Ohishi, K., Miyazaki, M., Fujita, M., Ogino, Y.: H^{∞} observer based force control without force sensor. In: Proceedings of International Conference on Industrial Electronics, Control and Instrumentation, pp. 1049–1054 (1991)
16. Ohishi, K., Miyazaki, M., Fujita, M., Ogino, Y.: Force control without force sensor based on mixed sensitivity H^{∞} design method. In: Proceedings of IEEE International Conference on Robotics and Automation, pp. 1356–1361 (1992)
17. Alcocer, A., Robertsson, A., Valera, A., Johansson, R.: Force estimation and control in robot manipulators. In: Proceedings of the 7^{th} Symposium on Robot Control (SYROCO 2003), pp. 31–36 (2003)
18. Kröger, T., Kubus, D., Wahl, F.M.: Force and acceleration sensor fusion for compliant manipulation control in 6 degrees of freedom. Advanced Robotics 21, 1603–1616 (2007)
19. Garcia, J.G., Robertsson, A., Ortega, J.G., Johansson, R.: Sensor fusion for compliant robot motion control. IEEE Transations on Robotics 24, 430–441 (2008)
20. Lichiardopol, S., van de Wouw, N., Nijmeijer, H.: Boosting human force: A robotic enhancement of a human operator's force. In: Proceedings of International Conference on Decision and Control, pp. 4576–4581 (2008)
21. Jiang, Z.P., Mareels, I.M.Y., Wang, Y.: A Lyapunov formulation of the nonlinear small-gain theorem for interconnected ISS systems. Automatica 32, 1211–1215 (1996)
22. Nešić, D., Teel, A.R., Sontag, E.D.: Formulas relating $\mathcal{KL}$-stability estimates of discrete-time and sampled-data nonlinear systems. Systems & Control Letters 38, 49–60 (1999)
23. Gielen, R., Olaru, S., Lazar, M., Heemels, W.P.M.H., van de Wouw, N., Niculescu, S.I.: On polytopic approximations as a modeling framework for systems with time-varying delays. Automatica (2010) (accepted)
24. Jiang, Z.P., Wang, Y.: Input-to-state stability for discrete-time nonlinear systems. Automatica 37, 857–869 (2001)